Journal of Quantitative Spectroscopy & Radiative Transfer 126 (2013) 84–90

Contents lists available at SciVerse ScienceDirect

Journal of Quantitative Spectroscopy & Radiative Transfer

journal homepage: www.elsevier.com/locate/jqsrt

Metallic nanoparticles in a standing wave: Optical force and heating

Martin Šiler*, Lukáš Chvátal, Pavel Zemánek

Institute of Scientific Instruments of the ASCR, v.v.i., Academy of Sciences of the Czech Republic, Královopolská 147, 612 64 Brno, Czech Republic

ARTICLE INFO

Article history:
Received 15 June 2012
Received in revised form
3 October 2012
Accepted 4 October 2012
Available online 16 October 2012

Keywords:
Metallic nanoparticles
Optical trapping
Heating
Generalized Lorenz–Mie theory

ABSTRACT

We have investigated the absorbed power in a single gold or silver metallic nanoparticle together with the optical force acting upon it if the particle is illuminated by two counter-propagating plane waves forming a standing wave. We have used the Generalized Lorenz–Mie theory (GLMT) and considered the incident wavelengths 250 nm $\leq \lambda_{vac} \leq$ 1250 nm and particles size parameter $0.1 \leq d/\lambda_{vac} \leq 4$. Similarly as in the case of dielectric particle we have found that the optical force is equal to zero for all particle positions in the standing wave for certain wavelengths and particle sizes. However, in the case of a metallic object this phenomenon occurs for considerably smaller particles and the conditions change considerably with the illuminating wavelength especially near the localized surface plasmon resonances. Similarly, we have found that the absorbed heat does not change with the position of the particle in the standing wave for certain wavelengths and particle sizes. These sizes generally differ from those giving zero optical force and, therefore, the particle can be trapped at the intensity maximum or minimum and in both cases its heating is maximal or minimal depending on the particle size.

1. Introduction

Metal nanoparticles become very popular objects of various studies due to their compatibility with biological tissues and utilization as contrast agents in various bioimaging techniques [1–3]. For many years the utilization of metal nanoparticles is investigated in the cancer treatment because the concentration of metal nanoparticles injected to the body increases in cancerous tissue. If the nanoparticles in such tissue are illuminated by light that penetrates sufficiently deep, the nanoparticles are heated and can damage the surrounding cancerous cells [4,5]. The light absorption varies significantly with the particles size, shape and the illuminating wavelength due to the collective oscillations of the electron gas known as the localized plasmons [6]. Except applications in a living tissue an individual nanoparticle can be considered as a localized nanosource of heat [7–9]. However, to serve this way its position should be controlled in a contactless manner to prevent heat dissipation through the handle. Since the magnetic field cannot be applied upon gold and silver nanoparticles, mechanical effects of light known as optical forces can be employed [10,11]. The origin of optical forces comes from the transfer of momentum from light to an object during the scattering of light by the object. Various geometries of laser beams have been developed to keep an object trapped in 3D [12]. The most popular geometry is known as the optical tweezers and it is based on a single tightly focused laser beam [10,13,14]. Except the optical tweezers [15] dielectric nanoparticles can be confined also in other geometries employing evanescent waves or counter-propagating beams [16–23]. Significant attention has been also paid to the optical manipulation with metallic particles using optical tweezers or evanescent waves [11,24–32]. However, only a few papers discussed the heating of optically trapped metallic nanoparticles [24–27,33]. In this paper

* Corresponding author. Tel.: +420 541514240.
E-mail address: siler@isibrno.cz (M. Šiler).
URL: http://www.isibrno.cz/omitec (M. Šiler).

0022-4073/$ - see front matter © 2012 Elsevier Ltd. All rights reserved.
http://dx.doi.org/10.1016/j.jqsrt.2012.10.005

we omit the thermophoretic forces [34] and focus only on the optical forces. Even though it has been pointed out that the standing wave provides much stronger axial optical confinement of dielectric nanoparticles [18,19,22], no investigation has been done on metallic nanoparticles to verify this conclusion. Therefore, in this paper we focused on the optical forces and associated heating of metallic spheres illuminated by two counter-propagating plane waves forming a standing wave.

2. Optical forces

We consider spherical particles of different sizes that are beyond the Rayleigh approximation and therefore we applied the generalized Lorenz–Mie theory (GLMT) [35–37], under equivalent Barton's version [38], to study the optical forces and heating of the metallic nanoparticles. The GLMT is based on the decomposition of the incident illuminating field into series of spherical harmonic functions Y_{lm} and getting the coefficients A_{lm} and B_{lm} of this expansion. Knowing these coefficients both the scattered field (described by coefficients a_{lm} and b_{lm}) and the optical forces can be evaluated. If the illumination is done by a plane wave, analytical form for the coefficients A_{lm} and B_{lm} exists [37]. Therefore, the optical forces can be expressed analytically and calculated numerically very fast even in the interference field of several plane waves, including the standing wave.

Due to the sinusoidal dependence of the optical intensity across the standing wave, i.e. z-axis, the profile of the optical force acting on a particle across the intensity fringes can be expressed as

$$F_z(z) = -F_{z0}\sin(2kz+\Phi_0), \tag{1}$$

where F_{z0} is the amplitude of the optical force along z-axis, $k = 2\pi n_{\text{ext}}/\lambda_{\text{vac}}$ is the magnitude of the wavevector $\mathbf{k}$; λ_{vac} and n_{ext} denote the vacuum wavelength and refractive index of the surrounding medium, respectively. Further, Φ_0 is the phase shift having two discrete values equal to 0 or π. It has been shown [39] that if $\Phi_0 = 0$ or $\Phi_0 = \pi$, the particle settles itself with its center to the bright high intensity or dark low intensity part of the interference fringe, respectively. This effect is called "size-effect" and is illustrated by blue curves and text in Fig. 1.

We performed a parametric study of the optical forces acting upon a single gold or silver particle of diameter d in the range $0.1 \le d/\lambda_{\text{vac}} \le 4$ if it is illuminated by two counter-propagating plane waves of vacuum wavelengths in the range $250 \le \lambda_{\text{vac}} \le 1250$ nm and identical intensities $E_0 = 6 \times 10^5$ V m^{-1}. This intensity value corresponds to the laser power of 1 mW passing through the area of 1 μm^2. The values of refractive indices of gold, silver, and water were taken from [40] for each considered wavelength.

Fig. 2 presents the results of numerical analysis of the calculated optical forces. For gold and silver particles the force amplitude F_{z0} and phase Φ_0 from Eq. (1) are shown here in a dependence on the particle size d/λ_{vac} and wavelength λ_{vac}. White contours denote such combinations of these parameters that give $F_{z0} = 0$, i.e. the optical force F_z is equal to zero at all axial positions z. These contours also serve as the border lines between sets of parameters where the particle is stably trapped either in the standing wave intensity maximum ($\Phi_0 = 0$) or minimum ($\Phi_0 = \pi$) as it is seen in Fig. 2(c, d). These areas form stripes, in the case of gold they are mainly parallel to the vertical axis, however, at wavelengths close to the plasmon resonance $\lambda_{\text{vac}} = 532$ nm their regular shape is disturbed. In the case of silver the zero force border lines are less organized and give more complex particles behavior comparing to gold particles. For example, tiny gold particles are always trapped at the intensity maximum for all investigated wavelengths but tiny silver particles are trapped at intensity minimum for 311 nm $< \lambda_{\text{vac}} < 400$ nm. It corresponds to the negative real part of the particle polarizability at these wavelengths [33]. The results also indicate that the particle behavior at the wavelengths close to the plasmon ones is more sensitive to the illuminating wavelength and particle size. This

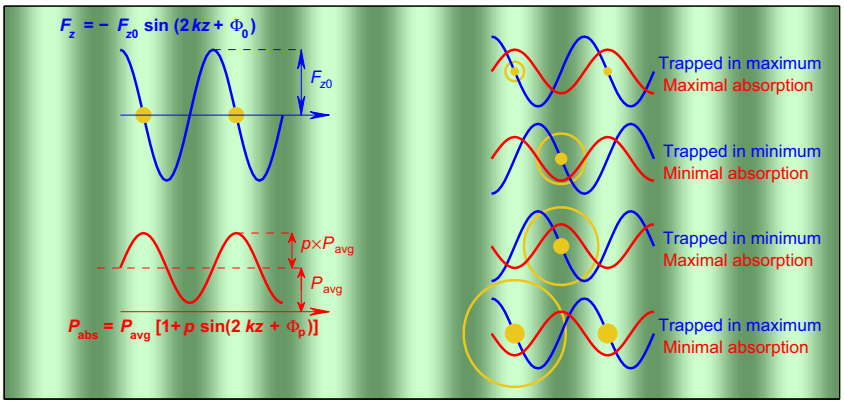

Fig. 1. A metal particle illuminated by a standing wave, optical forces acting upon the particle are blue, power absorbed by the particle is red. Depending on the particle size so-called "size-effect" in optical trapping occurs: the particle is confined with its center either at the intensity maximum (antinode of the standing wave) or minimum (standing wave node). Similarly the absorbed power (red curves) depends on the position where the particle is confined and leads to similar "size-effect" in particle heating. Yellow circles depict the approximate sizes of particles in each possible case. (For interpretation of the references to color in this figure caption, the reader is referred to the web version of this article.)

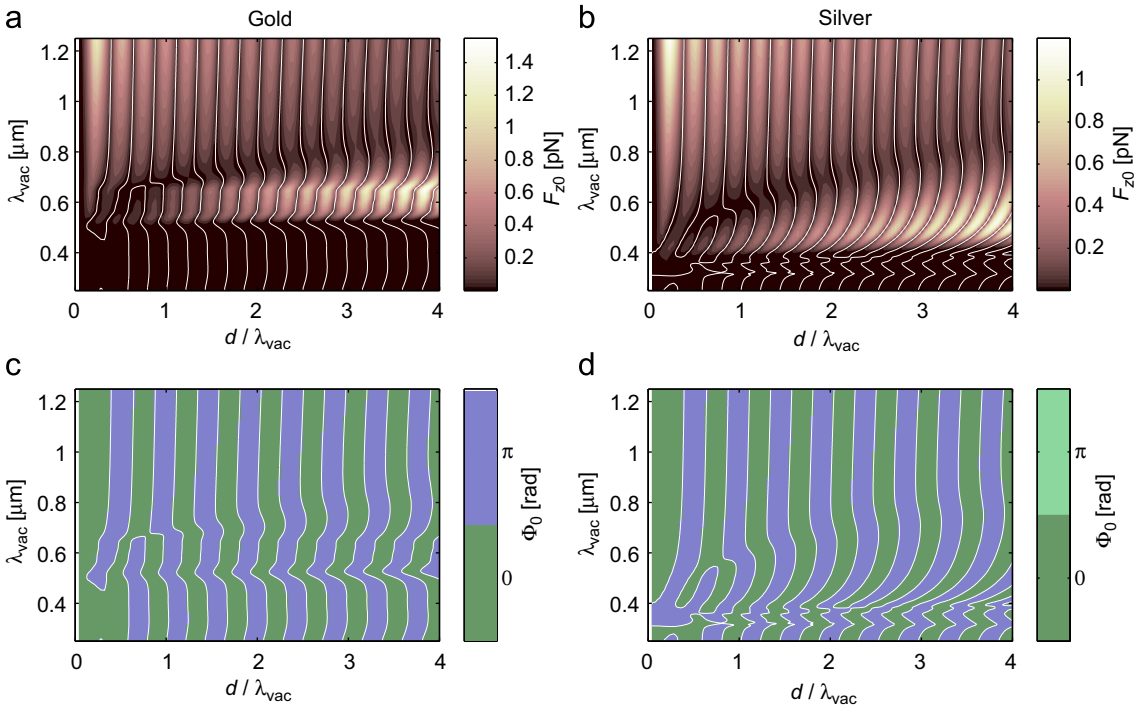

Fig. 2. Amplitude of the optical force F_{z0} and phase Φ_0 in the standing wave as the function of the illuminating wavelength λ_{vac} and the particle size (in units of d/λ_{vac}). Only the particles made of gold (a, c) and silver (b, d) were considered. The white curves denote the case when $F_{z0}=0$ for all particle positions z, i.e. such combination of parameters where the particle moves freely across the standing wave. $\Phi_0=0$ and $\Phi_0=\pi$ correspond to the particle confined at the standing wave intensity maximum or minimum, respectively. Electric field intensity of each counter-propagating plane waves was set to $E_0=6\times10^5$ V m^{-1} corresponding to the optical power of 1 mW passing through 1 μm m^2.

property could be used for size-sensitive sorting of metallic particles in one-dimensional optical lattices [41–44], structured near-field [32], or counter-propagating beams of different wavelengths [31].

3. Heating of metallic particles

Metallic particles have higher complex part of polarizability comparing to dielectric particles which leads to higher absorption of light and their stronger heating. To quantify the nanoparticle heating we used the GLMT [45] to calculate the total power absorbed by the spherical particle if illuminated by an arbitrary incident light field. However, the result given by Eq. (34) in Ref. [45] should be corrected by the missing medium refractive index. The correct formula (in SI units) follows:

$$P_{abs}=-\frac{1}{2}\omega k\sum_{l=1}^{\infty}\sum_{m=-l}^{l} l(l+1)[\epsilon|a_{lm}|^2+\mu_0|b_{lm}|^2 + \Re(\epsilon A_{lm}a_{lm}^*+\mu_0 B_{lm}b_{lm}^*)], \quad (2)$$

where ϵ is permittivity of the surrounding medium, μ_0 is vacuum permeability, $\Re(X)$ denotes the real part of X and coefficients A_{lm} and B_{lm} are defined using Eqs. (32) and (33) in Ref. [45]. We verified numerically the validity of corrected Eq. (2) using the finite element modeling of electromagnetic scattering in Comsol Multiphysics software. In the case of considered particle illumination by the standing wave, we assume the following form of the absorbed power:

$$P(z)=P_{avg}[1+p\cos(2kz+\Phi_p)], \quad (3)$$

where P_{avg} is the absorbed power averaged over one fringe, p gives the relative amplitude of modulation of the absorbed power over one standing wave fringe (i.e. $0\le p\le 1$), and Φ_p is the phase shift having values either 0 or π, similarly as Φ_0 in the case of optical force in Eq. (1). For example, the particle trapped at the intensity maximum (e.g. $z=0$) absorbs maximally for $\Phi_0=0$ and minimally for $\Phi_0=\pi$.

Fig. 3 presents the results of calculated absorbed power in gold and silver particles using the same set of independent variables as in Fig. 2. Fig. 3(a, b) reveals that larger particles in general absorb more power P_{avg} especially in the vicinity of the plasmon resonances. We have also calculated the absorption cross-section C_{abs} [46] for a particle illuminated by a single plane wave. We plotted a curve depicting a wavelength λ_{vac} for which C_{abs} is maximal for a fixed particle size d/λ_{vac}. This curve exactly matches with the maximal absorption depicted in Fig. 3(a, b). Moreover, a gold particle absorbs almost two times more power than silver one of the same size. Light absorption by smaller particles is more dependent on the particle position in the standing wave because the particle is well localized in between the interference fringes, see Fig. 3(c, d). For example if $p\simeq 1$ such particle absorbs very weakly if it is located at the intensity minimum. In case of larger particles, such modulation vanishes at short wavelengths while it is

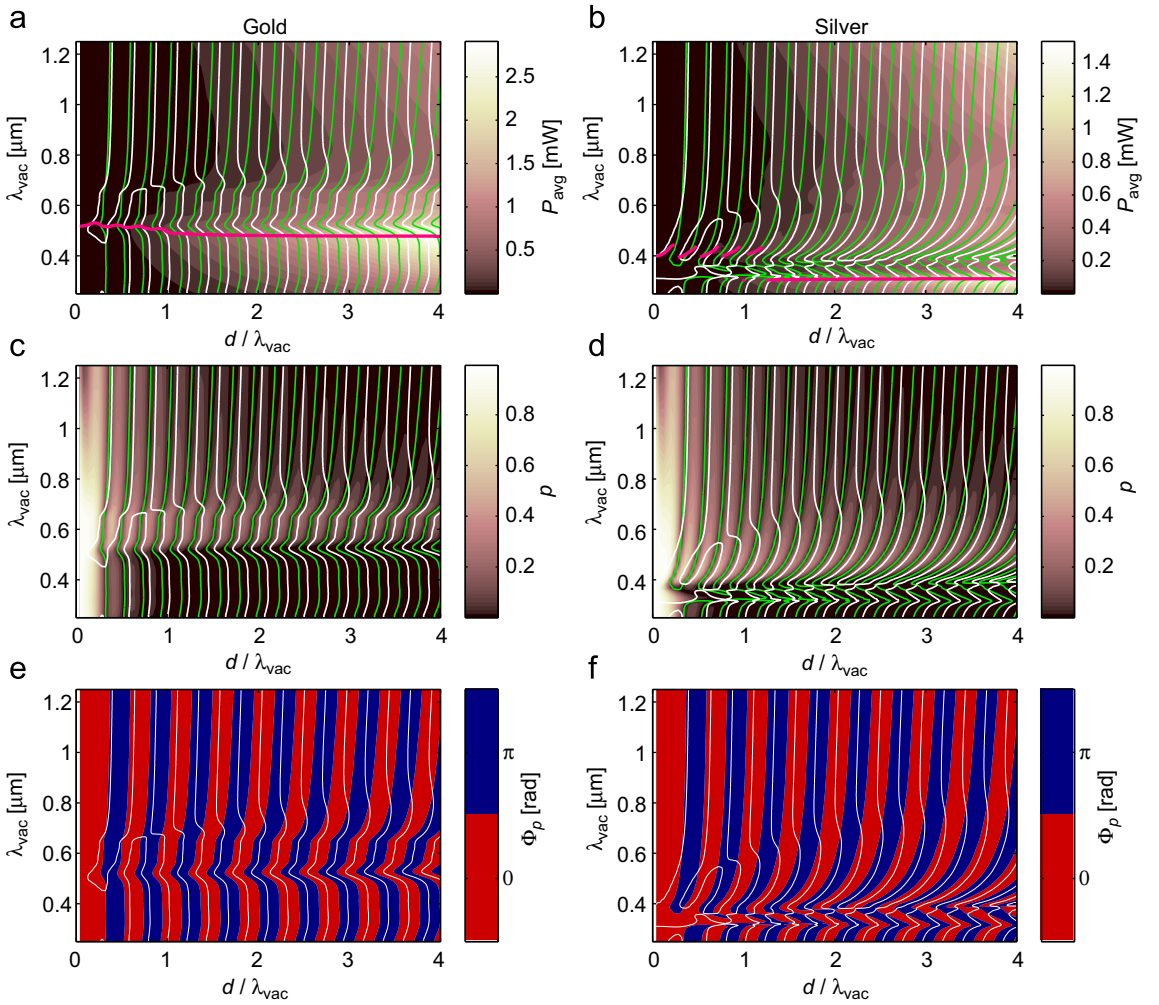

Fig. 3. Results of calculated power absorbed by gold (a, c, e) and silver (b, d, f) particle using the parameters of Eq. (3). The average absorbed power independent on the axial particle position P_{avg} is plotted in (a, b); the relative amplitude of the axial modulation of the absorbed power p is depicted in (c, d). The red and blue areas in (e, f) denote two discrete values of Φ_p. The green contours denote situation when $p=0$ and the white curves correspond to $F_{z0}=0$ from Fig. 2. The pink curves in (a, b) denote the wavelengths where the absorption cross-section C_{abs} reaches maximal values for fixed particle size parameter d/λ_{vac} (for single plane wave illumination). The independent variables λ_{vac} and d/λ_{vac} together with E_0 were the same as in Fig. 2. (For interpretation of the references to color in this figure caption, the reader is referred to the web version of this article.)

still present in a small extent for long wavelengths. Green curves denote the situation when the absorbed power does not depend on the z-position of the particle. Straightforward comparison in Fig. 3 reveals that there exist different combinations of parameters for which the optical force (white contours) and absorbed power (green curves) do not depend on the z-position of the particle. Fig. 1 shows all four distinct situations that can occur. The force and absorbed power profiles are shown by blue and red curves, respectively, the stable location of the particle is denoted by a dot and the approximate particle sizes are shown by yellow circles.

The absorbed power heats the particle and its temperature rises. Since the thermal conductivities of gold and silver are much higher than that of the surrounding media (κ), we may assume that the temperature is constant all over the particle volume, however, it decreases outside the particle following [26]:

$$T = T_0 + \Delta T \frac{a}{r}, \quad \Delta T = \frac{P}{2\pi d\kappa}, \tag{4}$$

where T_0 is the ambient temperature without the heat source, r is the distance from the particle center and P is the absorbed power.

Fig. 4(a, b) presents the increase of temperature on the particle surface if the particle is stably trapped. It clearly illustrates that the particle's surface temperature may overcome 100 °C and can prevent trapping of such particle. For comparison Fig. 4(c, d) shows that the difference between the surface temperatures of a particle located at the unstable and stable positions may exceed 100 °C, especially for small particles. In contrast, Fig. 4(c, d) also demonstrates that the positive difference $T_{unstable}-T_{stable}$ corresponds to the regimes where the particle absorbs

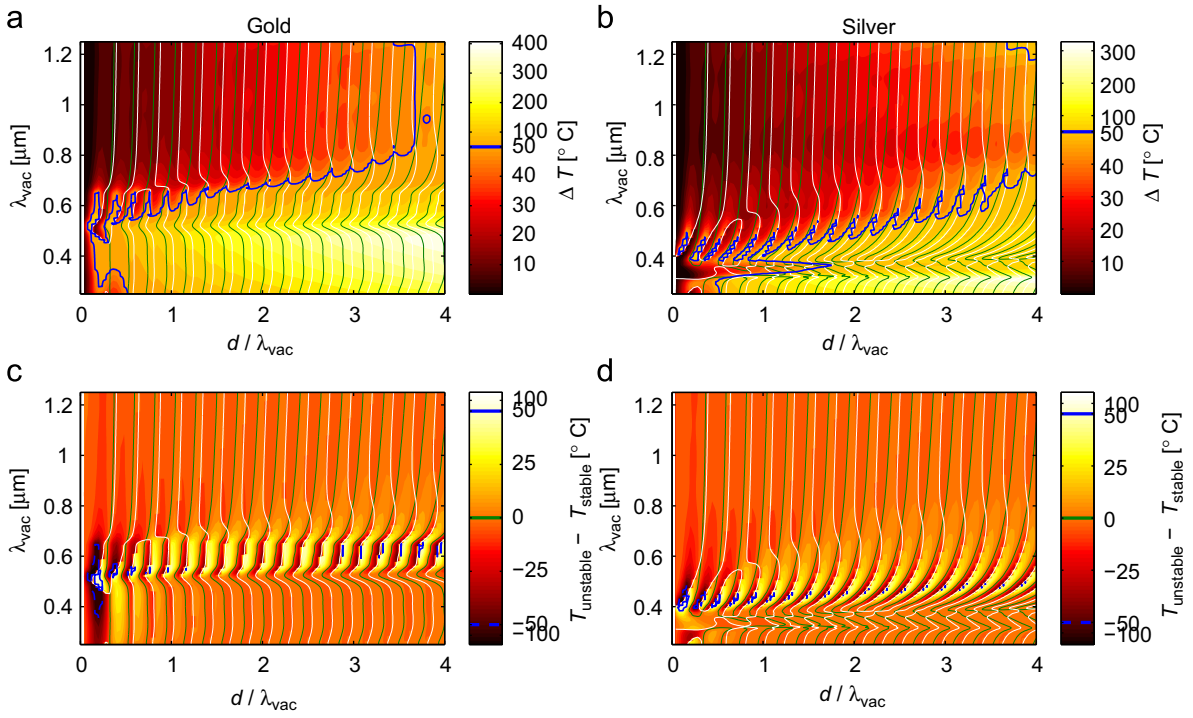

Fig. 4. Surface temperature increase ΔT of gold (a) and silver (b) particle caused by the absorbed light and given by Eq. (4). ΔT is calculated for the particle located at the stable position given by the optical force F_z. Figures (c) and (d) show the difference of the particle surface temperature if the particle is located at unstable and stable positions. Note that the pseudo-color scale is changed when the temperature rise reaches $\pm$ 50 °C (the areas of different color scales are separated by the blue curves). The white and green curves have the same meaning as in Fig. 3. (For interpretation of the references to color in this figure caption, the reader is referred to the web version of this article.)

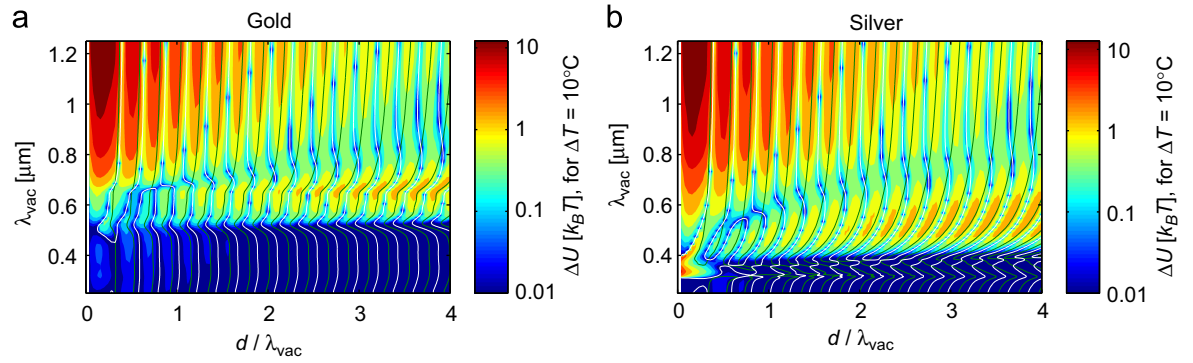

Fig. 5. Optical trap depth ΔU (in logarithmic scale) for gold (a) and silver (b) particles if they are heated by 10 °C.

less while being settled in its stable position. This indicates that even metallic particles could be optically trapped without their intense heating.

To verify this conclusion we calculated the incident trapping power necessary to heat up the particle by 10 °C and in Fig. 5 we draw the depth of the optical trap ΔU corresponding to this power. The trap depth ΔU is obtained from the work needed to transfer the particle from the equilibrium position to the edge of the trap and using Eq. (1) the axial optical potential profile $U_z(z)$ can be expressed as

$$U_z(z) = -\int F_z(z)\,\mathrm{d}z = -\frac{\Delta U}{2}\cos(2kz+\Phi_0). \tag{5}$$

We have chosen the temperature increase $\Delta T = 10$ °C so that both the particle motion and its surrounding liquid would not be strongly influenced by this temperature change. If we consider that the minimal trap depth should satisfy $\Delta U > 1 k_B T$ in order to influence the Brownian particle motion by light, only several combinations of

parameters satisfy this condition. The deepest optical traps are created for small gold and silver particles illuminated by longer wavelengths. There are no significant differences in the maximal trap depths comparing gold and silver particles. An interesting situation happens for tiny silver particles illuminated by wavelengths between 310 nm and 400 nm. They are confined at the intensity minimum with negligible absorption and heating. However, we have previously shown [47] that in order to keep the particle stably trapped for at least a minute without jumping to the neighboring potential well, the trap depth has to satisfy $\Delta U > 7.5 k_B T$. Looking at Fig. 5 this condition is fulfilled only for tiny particles trapped using long wavelengths (red to near infrared) or for silver nanoparticles trapped at the intensity minimum of the interference fringe.

4. Conclusion

We have studied the behavior of a single gold or silver particle placed in an interference field of two counter-propagating plane waves. We present the results of the parametric study that focused on the optical forces acting upon a single particle and the heat absorbed by a single particle placed at various positions across the interference fringe. We varied the illuminating wavelength and the particle size and we found that for particular sets of these parameters the axial optical force does not depend on the particle position in the standing wave. Due to the larger scattering cross-section of metal particles compared to the dielectric particles, this phenomenon occurs at smaller sizes of metal particles comparing to dielectric ones and it is much more sensitive to the particle size near the plasmon resonance. This could lead to efficient optical sorting of metal nanoparticles of different sizes. Similarly, there exist particular wavelengths and particle sizes for which the absorbed power does not change with the particle position at the intensity fringe. However, such sets of parameters are different comparing to those giving zero amplitude of axial optical force. Therefore, a metallic particle stably trapped at intensity maximum or minimum can absorb the power strongly or weakly depending on the parameters. If we limited the incident trapping power by maximal temperature increase of the confined gold or silver particle, only tiny particles may be trapped using red to near infrared wavelengths. However, silver nanoparticles may be also axially confined using shorter trapping wavelengths in the range of 310–400 nm because the particles polarizability is negative and the particles are confined at the intensity minimum of the standing wave.

Acknowledgment

The authors acknowledge the support from the Czech Science Foundation (GPP205/12/P868), Ministry of Education, Youth and Sports of the Czech Republic (LH12018) together with the European Commission (ALISI No. CZ.1.05/2.1.00/01.0017).

References

[1] Boisselier E, Astruc D. Gold nanoparticles in nanomedicine: preparations, imaging, diagnostics, therapies and toxicityChem Soc Rev 2009;38(6):1759–82. http://dx.doi.org/10.1039/b806051g.
[2] Jain PK, Huang X, Sayed El-IH, El-Sayed MA. Noble metals on the nanoscale: optical and photothermal properties and some applications in imaging, sensing, biology, and medicineAcc Chem Res 2008;41(12):1578–86. http://dx.doi.org/10.1021/ar7002804.
[3] Lal S, Link S, Halas NJ. Nano-optics from sensing to waveguiding. Nat Photonics 2007;1(11):641–8. http://dx.doi.org/10.1038/nphoton.2007.223.
[4] Huang X, Jain PK, Sayed El-IH, El-Sayed MA. Plasmonic photothermal therapy (PPTT) using gold nanoparticles. Lasers Med Sci 2008;23(3):217–28. http://dx.doi.org/10.1007/s10103-007-0470-x.
[5] Loo C, Lowery A, Halas N, West J, Drezek R. Immunotargeted nanoshells for integrated cancer imaging and therapy. NanoLett 2005;5(4):709–11. http://dx.doi.org/10.1021/nl050127s.
[6] Jain PK, Lee KS, Sayed El-IH, El-Sayed MA. Calculated absorption and scattering properties of gold nanoparticles of different size, shape, and composition: applications in biological imaging and biomedicineJ Phys Chem BAppl Biol Imaging Biomed. 2006;110(14):7238–48. http://dx.doi.org/10.1021/jp057170o.
[7] Merabia S, Keblinski P, Joly L, Lewis LJ, Barrat JL. Critical heat flux around strongly heated nanoparticles. Phys Rev E 2009;79(2, Part 1):021404. http://dx.doi.org/10.1103/PhysRevE.79.021404.
[8] Baffou G, Quidant R, de Abajo FJG. Nanoscale control of optical heating in complex plasmonic systems. ACS Nano 2010;4(2):709–16. http://dx.doi.org/10.1021/nn901144d.
[9] Baffou G, Girard C, Quidant R. Mapping heat origin in plasmonic structures. Phys Rev Lett 2010;104:136805.
[10] Ashkin A, Dziedzic JM, Bjorkholm JE, Chu S. Observation of a single-beam gradient force optical trap for dielectric particles. Opt Lett 1986;11:288–90.
[11] Svoboda K, Block SM. Optical trapping of metallic Rayleigh particles. Opt Lett 1994;19:930–2.
[12] Jonáš A, Zemánek P. Light at work: the use of optical forces for particle manipulation, sorting, and analysisElectrophoresis 2008;29:4813–51.
[13] Grier DG. A revolution in optical manipulation. Nature 2003;424:810–6.
[14] Fazal FM, Block SM. Optical tweezers study life under tension. Nat Photonics 2011;5:318–21.
[15] Smith T, Hotta J, Sasaki K, Masuhara H, Itoh Y. Photon pressure-induced association of nanometer-sized polymer chains in solution. J Phys Chem B 1999;103(10):1660–3.
[16] Chaumet P, Rahmani A, Nieto-Vesperinas M. Optical trapping and manipulation of nano-objects with an apertureless probe. Phys Rev Lett 2002;88:123601.
[17] Novotny L, Bian RX, Xie XS. Theory of nanometric optical tweezers. Phys Rev Lett 1997;79:645–8.
[18] Zemánek P, Jonáš A, Šrámek L, Liška M. Optical trapping of Rayleigh particles using a Gaussian standing wave. Opt Commun 1998;151:273–85.
[19] Zemánek P, Jonáš A, Jákl P, Šerý M, Ježek J, Liška M. Theoretical comparison of optical traps created by standing wave and single beam. Opt Commun 2003;220:401–12.
[20] Šiler M, Čižmár T, Jonáš A, Zemánek P. Surface delivery of a single nanoparticle under moving evanescent standing-wave illumination. New J Phys 2008;10:113010. http://dx.doi.org/10.1088/1367-2630.
[21] Šiler M, Zemánek P. Optical forces acting on a nanoparticles placed into an interference evanescent field. Opt Commun 2007;275:409–20.
[22] Šiler M, Zemánek P. Parametric study of optical forces acting upon nanoparticles in a single, or a standing, evanescent wave. J Opt 2011;13:044016.
[23] Albaladejo S, Marques MI, Scheffold F, Saenz JJ. Giant enhanced diffusion of gold nanoparticles in optical vortex fields. Nano Lett 2009;9(10):3527–31. http://dx.doi.org/10.1021/nl901745a.
[24] Ke P, Gu M. Characterization of trapping force on metallic Mie particles. Appl Opt 1999;38(1):160–7.
[25] Ito S, Yoshikawa H, Masuhara H. Laser manipulation and fixation of single gold nanoparticles in solution at room temperature. Appl Phys Lett 2002;80(3):482–4.
[26] Seol Y, Carpenter AE, Perkins TT. Gold nanoparticles: enhanced optical trapping and sensitivity coupled with significant heatingOpt Lett 2006;31(16):2429–31. http://dx.doi.org/10.1364/OL.31.002429.
[27] Dienerowitz M, Mazilu M, Dholakia K. Optical manipulation of nanoparticles: a reviewJ Nanophotonics 2008;2:021875.

[28] Bosanac L, Aabo T, Bendix PM, Oddershede LB. Efficient optical trapping and visualization of silver nanoparticles. NanoLett 2008;8(5):1486–91. http://dx.doi.org/10.1021/nl080490.
[29] Jones PH, Palmisano F, Bonaccorso F, Gucciardi PG, Calogero G, Ferrari AC, et al. Rotation detection in light-driven nanorotors. ACS Nano 2009;3(10):3077–84. http://dx.doi.org/10.1021/nn900818n.
[30] Juan ML, Righini M, Quidant R. Plasmon nano-optical tweezers. Nat Photonics 2011;5:349–56.
[31] Ploschner M, Čižmár T, Mazilu M, Di Falco A, Dholakia K. Bidirectional optical sorting of gold nanoparticles. Nano Lett 2012;12(4): 1923–7. http://dx.doi.org/10.1021/nl204378r.
[32] Cuche A, Stein B, Canaguier-Durand A, Devaux E, Genet C, Ebbesen TW. Brownian motion in a designer force field: dynamical effects of negative refraction on nanoparticlesNano Lett 2012;12(8): 4329–32. http://dx.doi.org/10.1021/nl302060t.
[33] Trojek J, Chvátal L, Zemánek P. Optical alignment and confinement of an ellipsoidal nanorod in optical tweezers: a theoretical studyJ Opt Soc Am A 2012;29(7):1224–36.
[34] Lewittes M, Arnold S, Oster G. Radiometric levitation of micron sized spheres. Appl Phys Lett 1982;40(6):455–7.
[35] Lock JA, Gouesbet G. Generalized Lorenz–Mie theory and applications. J Quant Spectrosc Radiat Transfer 2009;10(11, Sp. Iss. SI): 800–7. http://dx.doi.org/10.1016/j.jqsrt.2008.11.013.
[36] Gouesbet G, Lock J, Gréhan G. Generalized Lorenz–Mie theories and description of electromagnetic arbitrary shaped beams: localized approximations and localized beam models, a reviewJ Quant Spectrosc Radiat Transfer 2011;112:1–27.
[37] Gouesbet G, Gréhan G. Generalized Lorenz–Mie theories. Springer; 2011.
[38] Barton JP, Alexander DR, Schaub SA. Theoretical determination of net radiation force and torque for a spherical particle illuminated by a focused laser beam. J Appl Phys 1989;66:4594–602.
[39] Zemánek P, Jonáš A, Liška M. Simplified description of optical forces acting on a nanoparticle in the Gaussian standing wave. J Opt Soc Am A 2002;19:1025–34.
[40] Palik E, Ghosh G. Handbook of optical constants of solidsdot in handbook of optical constants of solids, vol. 3. Academic Press; 1998 ISBN 9780125444231.
[41] Čižmár T, Šiler M, Šerý M, Zemánek P, Garcés-Chávez V, Dholakia K. Optical sorting and detection of sub-micron objects in a motional standing wave. Phys Rev B 2006;74:035105.
[42] Ricárdez-Vargas I, Rodríguez-Montero P, Ramos-García R, Volke-Sepúlveda K. Modulated optical sieve for sorting of polydisperse microparticles. Appl Phys Lett 2006;88:121116.
[43] Jákl P, Čižmár T, Šerý M, Zemánek P. Static optical sorting in a laser interference field. Appl Phys Lett 2008;92(16):161110, http://dx.doi.org/10.1063/1.2913759.
[44] Tamura M, Iida T. Fluctuation-mediated optical screening of nanoparticles, Nano Lett 2012, published online. 10.1021/nl302716c.
[45] Barton JP, Alexander DR, Schaub SA. Internal and near-surface electromagnetic fields for a spherical particle irradiated by a focused laser beam. J Appl Phys 1988;64:1632–9.
[46] Bohren CF, Huffman DR. Absorption and scattering of light by small particles. New York: John Wiley & Sons; 1998.
[47] Šiler M, Zemánek P. Particle jumps between optical traps in a one-dimensional optical lattice. New J Phys 2010;12:083001.